Research Paper

In Vivo Targeting of Metabolically Labeled Cancers with Ultra-Small Silica Nanoconjugates

Hua Wang[1], Li Tang[1], Yang Liu[1], Iwona Teresa Dobrucki[2], Lawrence W. Dobrucki[3], Lichen Yin[4✉], Jianjun Cheng[1✉]

1. Department of Materials Science and Engineering, University of Illinois at Urbana-Champaign, Urbana, Illinois 61801, USA.
2. Molecular Imaging Laboratory, Beckman Institute for Advanced Science and Technology, University of Illinois at Urbana-Champaign, Urbana, Illinois 61801, USA.
3. Department of Bioengineering, University of Illinois at Urbana-Champaign, Urbana, Illinois 61801, USA.
4. Jiangsu Key Laboratory for Carbon-Based Functional Materials & Devices, Institute of Functional Nano & Soft Materials (FUNSOM), Collaborative Innovation Center of Suzhou Nano Science and Technology, Soochow University, Suzhou 215123, Jiangsu, China.

✉ Corresponding authors: jianjunc@illinois.edu, lcyin@suda.edu.cn.

Abstract

Unnatural sugar-mediated metabolic labeling of cancer cells, coupled with efficient Click chemistry, has shown great potential for *in vivo* imaging and cancer targeting. Thus far, chemical labeling of cancer cells has been limited to the small-sized azido groups, with the large-sized and highly hydrophobic dibenzocyclooctyne (DBCO) being correspondingly used as the targeting ligand. However, surface modification of nanomedicines with DBCO groups often suffers from low ligand density, difficult functionalization, and impaired physiochemical properties. Here we report the development of DBCO-bearing unnatural sugars that could directly label LS174T colon cancer cells with DBCO groups and subsequently mediate cancer-targeted delivery of azido-modified silica nanoconjugates with easy functionalization and high azido density *in vitro* and *in vivo*. This study, for the first time, demonstrates the feasibility of metabolic labeling of cancer cells with large-sized DBCO groups for subsequent, efficient targeting of azido-modified nanomedicines.

Key words: Click chemistry, cancer targeting, nanomedicine, silica nanoconjugate, multi-modal imaging.

Introduction

Nanomedicines have been extensively explored for medical applications because of their capabilities to enhance drug solubility, promote drug absorption, control drug release, and reduce side effects.[1-3] Numerous types of nanomedicines including liposomes, polymeric micelles, drug-polymer conjugates, and nanoparticles (NPs) have been developed, each possessing unique properties to meet specific therapeutic demands.[4-6] Among those nanomedicines, silica NP has been widely used and explored for drug delivery because of their great biocompatibility and optical transparency, easy size control, and facile surface functionalization.[7-11] Our group recently reported the development of silica-drug nanoconjugates (NCs) with precisely controlled size within the range of 20-200 nm, high drug loading, and controllable surface properties.[6,12,13] These silica NCs also enable easy multi-functionalization via versatile silane chemistries for *in vivo* multi-modal imaging and targeting applications.[14] We further unraveled that silica NCs with varying sizes behaved differently in tumor penetration and cellular uptake, resulting in distinct tumor accumulation profiles.[6] Apart from such size-dependent passive tumor targeting, efforts also have been made to realize the active cancer targeting effect of silica NCs via the incorporation of targeting ligands such as aptamers and antibodies.[14,15] However, the targeting efficiency was unsatisfactory, and the large-sized targeting ligand may impair the physiochemical and pharmacokinetic properties of silica NCs.

Metabolic glycoengineering process of unnatural sugars provides a powerful tool to label cell-surface glycans with chemical functional groups.[16-19] This sugar-mediated cell labeling, coupled with

bioorthogonal chemistry, has shown great potential for cancer targeting over the past few years via a two-step strategy.[20-22] Unnatural sugars carrying chemical functional groups were first delivered to and metabolized in cancers, followed by the targeting of corresponding ligands that can react with the introduced functional groups in the second step. Among the efficient chemistries developed, copper-free Click chemistry between azide and dibenzocyclooctyne (DBCO) is most widely used, in particular *in vivo*, because of its high reaction rate and desired bioorthogonality and biocompatibility.[23-26] Multiple studies on the combination of azido-sugar labeling and Click chemistry have demonstrated its advantages in high targeting efficiency, absence of immunogenicity, and easy manufacturing.[27-31] For example, Kim et al.[32] reported that azido-sugar mediated labeling of tumor cells with azido groups could improve the tumor accumulation of DBCO-modified, drug-loaded chitosan nanoparticle. Chen group[33] also reported the use of azido-sugar loaded liposomes for cancer labeling and targeting. In all of these studies, metabolic labeling of cancer cells was limited to azido groups, and DBCO was used as the corresponding targeting ligand. However, due to the large size and great hydrophobicity of DBCO, functionalization of nanoparticles with DBCO often leads to low ligand density that will ultimately impede cancer targeting.[27,32] Efforts to improve the ligand density would compromise the water-solubility and other physiochemical properties of nanoparticles. To address such challenges, herein we developed a strategy to directly label cancer cells with DBCO groups and evaluated whether the expressed DBCO groups could significantly improve the tumor accumulation of azido-modified silica NCs. Considering its smaller size and lower hydrophobicity than DBCO, azido group could be easily introduced to the surface of silica NCs at a notably higher density and thus can potentially impart a higher cancer-targeting efficiency via Click chemistry.

Materials and Methods

Materials. D-Mannosamine hydrochloride and other materials were purchased from Sigma-Aldrich (St. Louis, MO, USA) unless otherwise noted. DBCO-NHS was purchased from Click Chemistry Tools (Scottsdale, AZ, USA). Cy5-azide was purchased from Kerafast (Boston, MA, USA). Azido-PEG-NHS (MW 3400) was purchased from Nanocs (New York, NY, USA). Sulfo-Cy5-NHS was purchased from Lumiprobe Corporation (Hallandale Beach, Florida, USA). DOTA-NHS was purchased from Macrocyclics Inc. (Dallas, TX, USA). Anhydrous

dimethylformamide (DMF) was purified by alumina columns and stored in the presence of molecular sieves.

Cell culture. LS174T colon cancer cell line was purchased from American Type Culture Collection (Manassas, VA, USA) and cultured in Dulbecco's Modified Eagle Medium (DMEM, Invitrogen, Carlsbad, CA, USA) containing 10% fetal bovine serum (FBS, Lonza Walkersville Inc, Walkersville, MD, USA), 100 units/mL Penicillin G, and 100 μg/mL streptomycin (Invitrogen, Carlsbad, CA, USA) at 37°C in 5% CO_2 humidified air.

Animals. Female 01B74 athymic nude mice were purchased from Charles River (Wilmington, MA, USA). Feed and water were available ad libitum. Artificial light was provided in a 12/12 hour cycle. The animal study protocol was reviewed and approved by the Illinois Institutional Animal Care and Use Committee (IACUC) of University of Illinois at Urbana-Champaign.

Instrumentation. Nuclear magnetic resonance (NMR) analyses were conducted on a Varian U500 (500 MHz) or a VXR500 (500 MHz) spectrometer. HPLC analyses were performed on a Shimadzu CBM-20A system (Shimadzu, Kyoto, Japan) equipped with a SPD20A PDA detector (190 nm-800 nm), an RF10Axl fluorescence detector, and an analytical C18 column (Shimadzu, 3 μm, 50*4.6 mm, Kyoto, Japan). Infrared spectra were recorded on a PerkinElmer 100 serial FTIR spectrophotometer. Scanning electron microscope (SEM) images were collected on a Hitachi S-4700 high resolution SEM. Confocal laser scanning microscopy (CLSM) images were taken on a Zeiss LSM 700 confocal microscope (Carl Zeiss, Thornwood, NY, USA). Flow cytometry analyses of cells were conducted with a BD FACS Canto 6-color flow cytometry analyzer (BD, Franklin Lakes, NJ, USA). *In vivo* and *ex vivo* fluorescence images of mice were taken on Bruker Xtreme In-Vivo Imaging System (Bruker, Billerica, MA, USA). Frozen tissues were embedded in the optimum cutting temperature (O.C.T.) compound (Sakura Finetek USA, Torrance, CA, USA), sectioned by a Leica CM3050S Cryostat and mounted on a glass slide. Micro-PET/CT imaging of mice was performed with small animal on a Siemens Inveon PET-CT system (Siemens Healthcare, Germany). *Ex vivo* measurement of radioactivity was conducted on a 2480 Wizard2 Automatic Gamma Counter (PerkinElmer, Waltham, MA, USA).

Synthesis of Ac₄ManDBCO. D-Mannosamine hydrochloride (2.0 mmol) and triethylamine (2.0 mmol) were dissolved in methanol (40 mL), followed by the addition of DBCO-NHS (2.0 mmol) in methanol. The mixture was stirred at room temperature for 24 h. Solvent was removed under

reduced pressure and the residue was redissolved in pyridine. Acetic anhydride (10 mL) was added and the reaction mixture was stirred at room temperature for another 24 h. After removal of the solvent, the crude product was purified by silica gel column chromatography using ethyl acetate/hexane (1/3, v/v) as the eluent to yield a white solid (55% yield). ^{1}H NMR (CDCl$_3$, 400 MHz): δ (ppm) 7.29-7.44&7.68 (m, 8H, Ph), 6.40&6.98 (dd, 1H, C(O)N*H*CH), 5.91&6.03 (dd, 1H, NHCHC*H*O), 5.26-5.30&5.08-5.12 (ddd, 1H, CH$_2$CHC*H*CH), 5.16-5.24 (dt, 1H, CH$_2$CHCHC*H*), 4.51-4.58 (m, 1H, NHC*H*CHO), 4.13-4.27 (m, 2H, C*H*$_2$CHCHCH), 3.98-4.05 (m, 1H, CH$_2$C*H*CHCH), 3.67 (t, 2H, NC*H*$_2$Ph), 2.74 (m, 2H, NHC(O)CH$_2$C*H*$_2$C(O)N), 2.56 (m, 2H, NHC(O)C*H*$_2$CH$_2$C(O)N), 2.03&2.07&2.10&2.15 (s, 12H, C*H*$_3$C(O)). LRMS (ESI) *m/z*: calculated for C$_{33}$H$_{34}$N$_2$O$_{11}$Na [M + Na]$^+$ 657.2, found 657.0.

Synthesis of Cy5-silane, azido-PEG$_{3.4k}$-silane and DOTA-silane. Sulfo-Cy5-NHS or azido-PEG$_{3.4k}$-NHS or DOTA-NHS (0.03 mmol) was dissolved in anhydrous DMF, followed by the addition of (3-aminopropyl)trimethoxysilane (0.03 mmol) and triethylamine (0.01 mmol) in DMF. The mixture was stirred at 45°C for 24 h, at which time point HPLC showed complete consumption of the starting materials. After removal of the solvent, the crude product was directly used without further purification.

Preparation and characterization of azido-/Cy5-NCs and Cy5-NCs. Azido-/Cy5-NCs were prepared following the reported procedures.[12] Methanol (1.0 mL), deionized water (0.36 mL), and concentrated ammonia (90 µL) were well mixed. Tetraethyl orthosilicate (TEOS) was added in one portion, followed by the addition of Cy5-silane (1 mg) in methanol (50 µL). The mixture was stirred at 100 rpm for 12 h. DOTA-silane (1 mg) and azido-PEG$_{3.4k}$-silane (1 mg) in methanol were then sequentially added, and the mixture was stirred for another 12 h. NCs were collected via centrifugation at 15000 rpm, washed with ethanol (1 mL × 3), and suspended in ethanol before storage at 4°C. Cy5-NCs without azido modification were prepared similarly except that azido-PEG$_{3.4k}$-silane was replaced with mPEG$_{3.4k}$-silane. The morphology and size of azido-/Cy5-NCs and Cy5-NCs were determined by S-4700 high resolution SEM. For fluorescence measurement, azido-/Cy5-NCs or Cy5-NCs in ethanol were collected via centrifugation, resuspended in deionized water, and measured on a fluorescence spectrometer.

Preparation and stability evaluation of ^{64}Cu-/azido-/Cy5-NCs and ^{64}Cu-/Cy5-NCs. ^{64}Cu chloride (obtained from Washington University, St. Louis, MO, USA) was mixed with azido-/Cy5-NCs or Cy5-NCs (2 mg, bearing DOTA moiety) in the NH$_4$OAc buffer solution (0.1 M, pH = 5.5, 1 mL). The mixture was vigorously stirred at 80°C for 1 h. ^{64}Cu-/azido-/Cy5-NCs or ^{64}Cu-/Cy5-NCs were collected via centrifugation at 15000 rpm and washed twice with PBS. To evaluate the serum stability, ^{64}Cu-/azido-/Cy5-NCs or ^{64}Cu-/Cy5-NCs were suspended in 10% FBS and distributed in 9 separate eppendorf tubes. Each solution was measured for the radioactivity (R$_{original}$) and incubated at 37°C. At selected time points (1, 3, and 6 h), ^{64}Cu-/azido-/Cy5-NCs or ^{64}Cu-/Cy5-NCs in triplicate tubes were collected via centrifugation and measured for the remaining radioactivity (R$_{remaining}$). The loss of ^{64}Cu from ^{64}Cu-/azido-/Cy5-NCs or ^{64}Cu-/Cy5-NCs was calculated by: (R$_{original}$- R$_{remaining}$) × 100%/R$_{original}$.

In vitro **cell labeling study**. To allow qualitative observation of the cell labeling efficiency, LS174T cells were seeded onto coverslips in a 6-well plate with a cell density of 40 k/well. Ac$_4$ManDBCO (20 µM) was added and incubated with cells at 37°C for 72 h. After washing with PBS, Cy5-azide (20 µM) in Opti-MEM was added and the cells were incubated for another 1 h. Paraformaldehyde (PFA) solution (4%, w/v) was added to fix the cells, and the cell nuclei were stained with DAPI (2 µg/mL). The coverslips were mounted on microscope slides with the addition of ProLong Gold antifade reagent (Life Technologies, Carlsbad, CA, USA) and the prepared samples were stored in dark for confocal imaging.

For quantitative analysis, LS174T cells cultured in a 24-well plate at an initial cell density of 10 k/well were incubated with Ac$_4$ManDBCO (20 µM) for 72 h, followed by treatment with Cy5-azide (20 µM) at 37°C for 1 h as described above. Cells were then washed, collected, and subjected to flow cytometry measurements. Data analysis was performed with the FCS Express software.

Cell uptake study of azido-/Cy5-NCs and Cy5-NCs. LS174T cells were cultured in 24-well plates and treated with Ac$_4$ManDBCO (20 µM) for 72 h. Cells without Ac$_4$ManDBCO treatment were used as controls. Azido-/Cy5-NCs or Cy5-NCs were added and incubated with cells for different time (0.5, 1, and 2 h) before assessment by flow cytometry.

Micro-PET/CT imaging. LS174T tumor models were established in 6 week-old female 01B74 athymic nude mice by subcutaneous injection of LS174T cells (1.5 million) in HBSS/matrigel (1/1, v/v) into both flanks. When the tumors reached ~50 mm^3, Ac$_4$ManDBCO (5 mg/kg) was intratumorally injected into the left tumors once daily for three days (Day 1-3), while the right tumors were injected with PBS as

controls. On Day 4, ^{64}Cu-/azido-/Cy5-NCs or ^{64}Cu-/Cy5-NCs (100 μL, ~100 μCi) were intravenously (i.v.) injected. At selected time intervals (1, 6 and 24 h post injection of NCs), mice were placed on the micro-CT imaging bed and kept anesthetized with a constant isoflurane flow. The micro-CT scan (80 KeV/500 μA X-ray energy, 360 projections, 360 degrees, 75 μm pixel size) was performed to determine the anatomical localization of tumors. Static micro-PET scans were acquired together with micro-CT scans for anatomical co-registration. The obtained micro-PET and micro-CT images were reconstructed with existing commercial software (Inveon Acquisition Workplace). Micro-PET images were processed using 3-D median filtering and fused with micro-CT images. Radioactivity in the selected regions of interest (ROIs) was quantified using the software and presented as the percentage of injected dose per gram tissue (% I.D./g).

Radioactivity measurement with γ-counter. Mice were euthanized and dissected after the last PET/CT scan. Major organs and tumors were harvested, weighed and measured for the ^{64}Cu radioactivity on a Wizard2 automatic γ-counter using appropriate energy window at photopeak of 511 KeV. Raw counts were corrected for background, decay, and weight, and converted to microcurie (μCi) per gram tissue via a previously established calibration curve. The radioactivity in each sample was presented as % I.D./g.

In vivo **and** *ex vivo* **fluorescence imaging**. LS174T tumor models were established in 6 week-old female 01B74 athymic nude mice by subcutaneous injection of LS174T cells (1.5 million) into both flanks. When the tumors reached ~100 mm³, Ac$_4$ManDBCO (5 mg/kg) was intratumorally injected into the left tumors once daily for three days (Day 1-3). The right tumors were injected with PBS as controls. On Day 4, azido-/Cy5-NCs or Cy5-NCs (200 mg/kg) were i.v. injected and its biodistribution was monitored via *in vivo* fluorescence imaging. Mice were placed on the sample stage equipped with anesthesia input and output ports, and imaged by the Bruker Xtreme In-Vivo Imaging System at selected time points (1, 6, 24, 48, and 72 h post i.v. injection of NCs). The excitation filter was set at 630 nm and the emission filter was set at 700 nm. Collected images were analyzed by the Bruker molecular imaging software. Major organs and tumors were harvested from mice at 72 h post injection of azido-/Cy5-NCs or Cy5-NCs, and imaged using the Bruker Xtreme In-Vivo Imaging System. *Ex vivo* images were quantified by measuring the fluorescence intensity at selected ROIs, and all values were expressed as mean ± standard deviation (n=3). After *ex vivo* imaging, tumors were

immediately frozen in O.C.T. compound and sectioned with a thickness of 8 μm on a cryostat (Leica CM3050S). DAPI in PBS (2 μg/mL) was added onto the tissue sections to stain the cell nuclei. After washing with PBS for three times, tissue sections were imaged under a fluorescence microscope.

In another set of experiments, after the intratumoral injection of Ac$_4$ManDBCO or PBS once daily for three days, tumors were harvested and sectioned with a thickness of 8 μm. Cy5-azide (10 μM) was added onto the tissue sections and incubated at 37°C for 30 min. After multiple washing steps, DAPI in PBS (2 μg/mL) was added to stain the cell nuclei. After washing with PBS, tissue sections were imaged under a fluorescence microscope.

Statistical analyses. Statistical analyses were conducted by Student's t-test (two-tailed) comparisons at 95% confidence interval. The results were deemed significant at $0.01 < *P \le 0.05$, highly significant at $0.001 < **P \le 0.01$, and extremely significant at $***P \le 0.001$.

Results and discussion

Ac$_4$ManDBCO mediated labeling of cancer cells *in vitro*

We first synthesized Ac$_4$ManDBCO by the coupling reaction between D-mannosamine and DBCO-NHS. The DBCO group of Ac$_4$ManDBCO is four carbons away from the sugar backbone, reaching a good balance between steric hindrance and change in the molecular weight of sugar moiety. We then studied whether Ac$_4$ManDBCO could metabolically label cancer cells with DBCO groups *in vitro*. LS174T colon cancer cells were incubated with Ac$_4$ManDBCO for three days, and the potentially expressed DBCO groups on the cell surface were detected by incubation with Cy5-azide for 30 min (Fig. 1a). As shown in Fig. 1b, LS174T cells treated with Ac$_4$ManDBCO showed strong Cy5 fluorescence intensity on the cell surface, indicating the successful expression of DBCO groups (Fig. S1). The control cells treated with PBS and further incubated with Cy5-azide, however, showed negligible Cy5 signals on the cell surface (Fig. 1b). Flow cytometry analyses of LS174T cells following the same treatment consistently showed much stronger Cy5 fluorescence intensity in Ac$_4$ManDBCO group than in PBS group (Fig. 1c-d). These results collectively demonstrated that Ac$_4$ManDBCO was able to metabolically label LS174T cancer cells with DBCO groups *in vitro*.

In order to study whether the cell-surface DBCO groups could mediate the targeted delivery of silica NCs with azido groups on surface, we designed Cy5- and DOTA-embedded, azido-modified silica NCs (azido-/Cy5-NCs) that not only enable PET/CT and

fluorescence dual-modal imaging but can also target the cell-surface DBCO groups via Click chemistry (Fig. 2a). We first synthesized Cy5-silane, azido-PEG$_{3.4k}$-silane, and DOTA-silane that can bind a radionuclide (^{64}Cu), and then prepared azido-/Cy5-NCs using the Stöber method (Fig. 2a). During the preparation of silica NCs, Cy5-silane was added shortly after the addition of tetraethyl orthosilicate (TEOS) to form a Cy5-filled silica core. DOTA-silane and azido-PEG$_{3.4k}$-silane were then added to display the DOTA moieties on the surface of silica NCs to bind ^{64}Cu and place the azido groups on the outermost surface of silica NCs to facilitate Click chemistry with DBCO groups on cell membranes (Fig. 2a). The control silica NCs without azido modification were synthesized similarly except that azido-PEG$_{3.4k}$-silane was replaced with mPEG$_{3.4k}$-silane. The size of silica NCs was well controlled, and we selected NCs with a diameter of ~50 nm for this study, considering its superior tumor accumulation compared to other sizes.[6] SEM and TEM images of azido-/Cy5-NCs showed the spherical morphology with a diameter of 48.8 ± 4.9 nm (Fig. 2b, Fig. S2). Azido-/Cy5-NCs could be well dispersed in PBS and were strongly fluorescent, with a maximum emission wavelength of 668 nm (Fig. 2c). Infrared spectrum of azido-/Cy5-NCs showed a peak at 2104 cm^{-1} (Fig. 2d), which verified the successful incorporation of azido groups. ^{64}Cu binding of azido-/Cy5-NCs or Cy5-NCs was achieved with high efficiency, and the resulting ^{64}Cu-/azido-/Cy5-NCs or ^{64}Cu-/Cy5-NCs showed desired stability in serum (Fig. 2e).
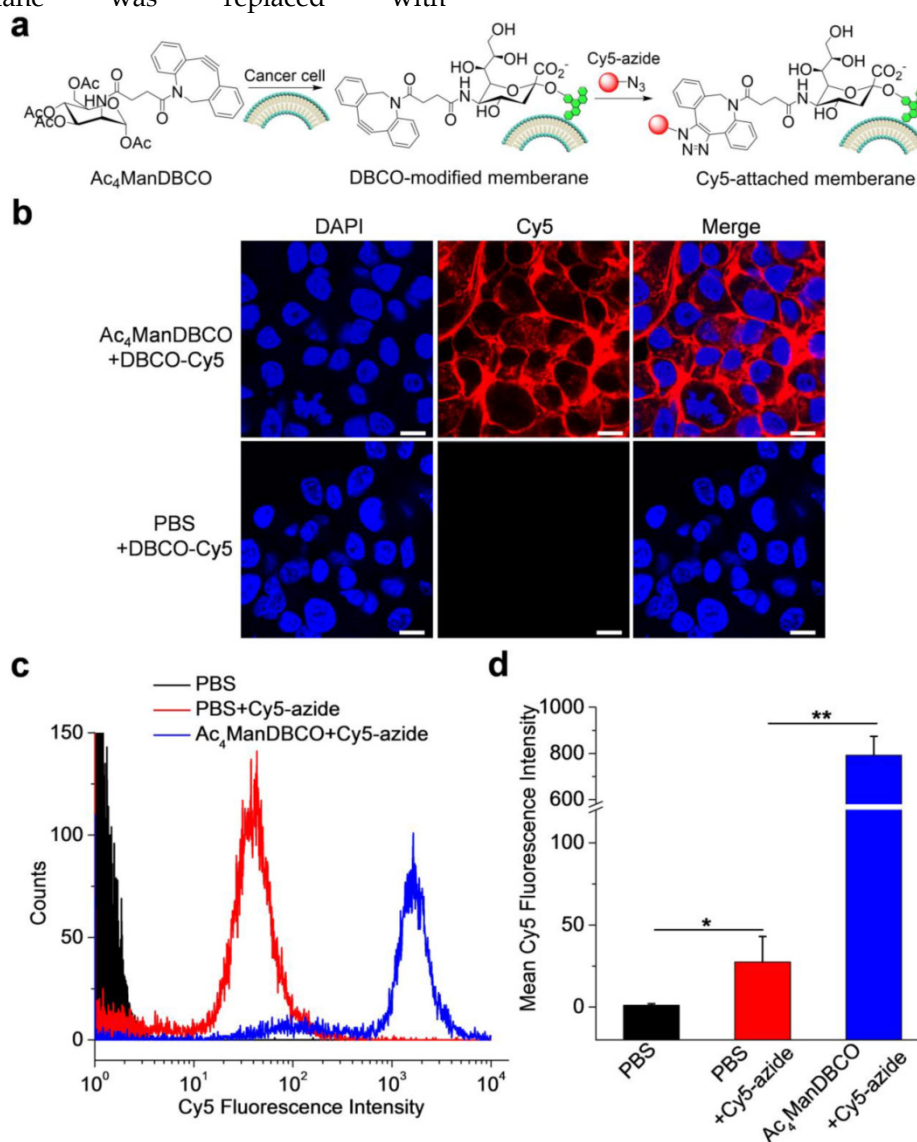
Figure 1. (a) Schematic illustration of Ac$_4$ManDBCO-mediated metabolic labeling of cancer cells and subsequent detection of cell-surface DBCO groups using Cy5-azide via copper-free Click chemistry. (b) CLSM images of LS174T cells after treatment with Ac$_4$ManDBCO (20 μM) or PBS for three days and further incubation with Cy5-azide (20 μM) for 30 min. Cell nuclei were stained with DAPI (blue). Scale bar represents 10 μm. (c) Flow cytometry analyses of LS174T cells following the same treatment in (b). (d) Mean Cy5 fluorescence intensity of LS174T cells extracted from (b). Data were presented as mean ± SEM (n=3) and analyzed by Student's t-test (two-tailed) (0.01 < *P ≤ 0.05, and 0.001 < **P ≤ 0.01).
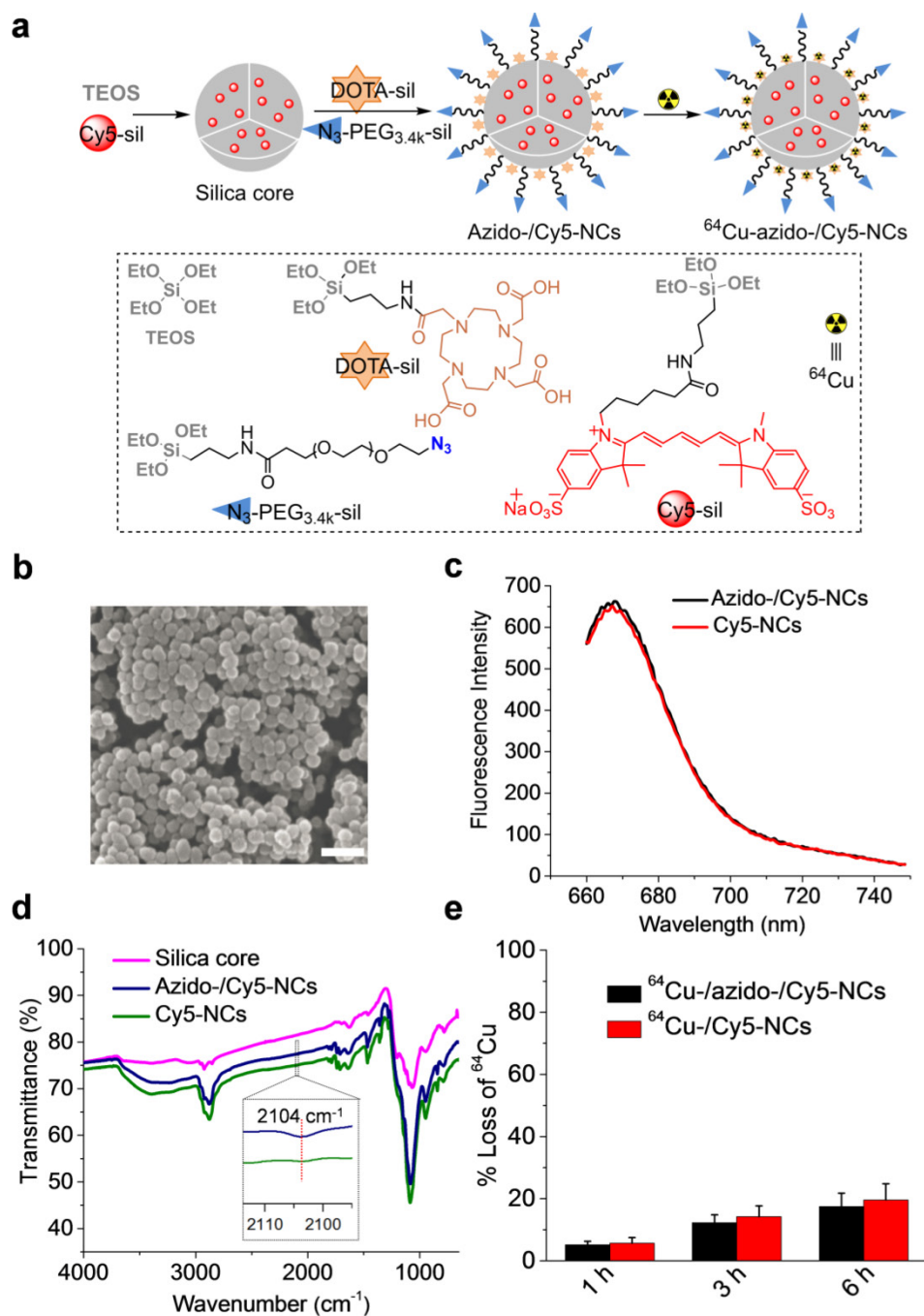
Figure 2. (a) Schematic illustration of the preparation of azido-/Cy5-NCs and ^{64}Cu-/azido-/Cy5-NCs. The chemical structures of TEOS, DOTA-silane, Cy5-silane, and azido-PEG$_{3.4k}$-silane were shown. Cy5-NCs and ^{64}Cu-/Cy5-NCs were synthesized similarly except that azido-PEG$_{3.4k}$-silane was replaced with mPEG$_{3.4k}$-silane. (b) SEM image of azido-/Cy5-NCs showed a size of 48.8 ± 4.9 nm. Scale bar represents 200 nm. (c) Fluorescence spectra of azido-/Cy5-NCs and Cy5-NCs. The excitation wavelength was set at 650 nm. (d) FTIR spectra of silica core, azido-/Cy5-NCs and Cy5-NCs. Inset: enlarged view of transmittance profiles of azido-/Cy5-NCs and Cy5-NCs within the wavenumber range of 2095-2114 cm^{-1}. (e) Loss of ^{64}Cu over time from ^{64}Cu-/azido-/Cy5-NCs or ^{64}Cu-/Cy5-NCs following incubation at 37°C in 10% FBS (n=3).

## Cell uptake of azido-/Cy5-NCs in DBCO-modified cancer cells

We next studied whether metabolic labeling of LS174T cells with DBCO groups would mediate the targeted delivery of azido-/Cy5-NCs via Click chemistry (Fig. 3a). LS174T cells were treated with Ac$_4$ManDBCO or PBS for three days and further incubated with azido-/Cy5-NCs for 30 min. Flow cytometry analyses showed significantly enhanced Cy5 fluorescence intensity in cells treated with Ac$_4$ManDBCO compared to control cells treated with PBS (Fig. 3b), which substantiated that Click chemistry-mediated active cell targeting notably promoted the cellular uptake of azido-/Cy5-NCs in DBCO-modified cells. A further time-dependent uptake study revealed that the internalization of azido-/Cy5-NCs in Ac$_4$ManDBCO-treated cells

occurred at a much faster rate than in PBS-treated control cells (Fig. 3c). Majority of the azido-/Cy5-NCs were taken up by Ac4ManDBCO-treated cells upon 30-min incubation, which suggested that the covalent binding of azido/Cy5-NCs with cell-surface DBCO groups was largely completed within 30 min. In comparison, azido/Cy5-NCs were gradually internalized in PBS-treated control cells within the 2-h incubation time, indicating the much faster targeted internalization of azido-/Cy5-NCs via Click chemistry than the non-targeted internalization. It is noteworthy that the uptake kinetics of Cy5-NCs in DBCO-modified cells was similar to that of azido-Cy5-NCs in unmodified cells (Fig. 3c), which excluded the effect of DBCO modification on the membrane permeability of cancer cells. Considering the highly mobile cell environment *in vivo*, Click chemistry-mediated targeted internalization of azido-/Cy5-NCs might impart a significant targeting effect.

## Click chemistry-mediated cancer targeting of azido-/Cy5-NCs *in vivo*

After demonstrating that Ac4ManDBCO-mediated chemical labeling of LS174T cells could markedly improve the cellular uptake of azido-/Cy5-NCs *in vitro*, we next studied whether Ac4ManDBCO could also label LS174T cancer cells *in vivo* and improve the tumor accumulation of azido-/Cy5-NCs. LS174T tumors were established in athymic nude mice by subcutaneous injection of LS174T cells into both flanks. When the tumors reached ~50 mm³, Ac4ManDBCO (5 mg/kg) was intratumorally (i.t.) injected into the left tumors once daily for three days (Day 1-3), while the right tumors were i.t. injected with PBS as controls. Confocal imaging of tissue sections of Ac4ManDBCO-treated tumors after being labeled with Cy5-azide showed significantly enhanced Cy5 signal compared to PBS-treated tumors (Fig. S3), which indicated the successful metabolic expression of DBCO groups. In another set of experiments, on Day 4,
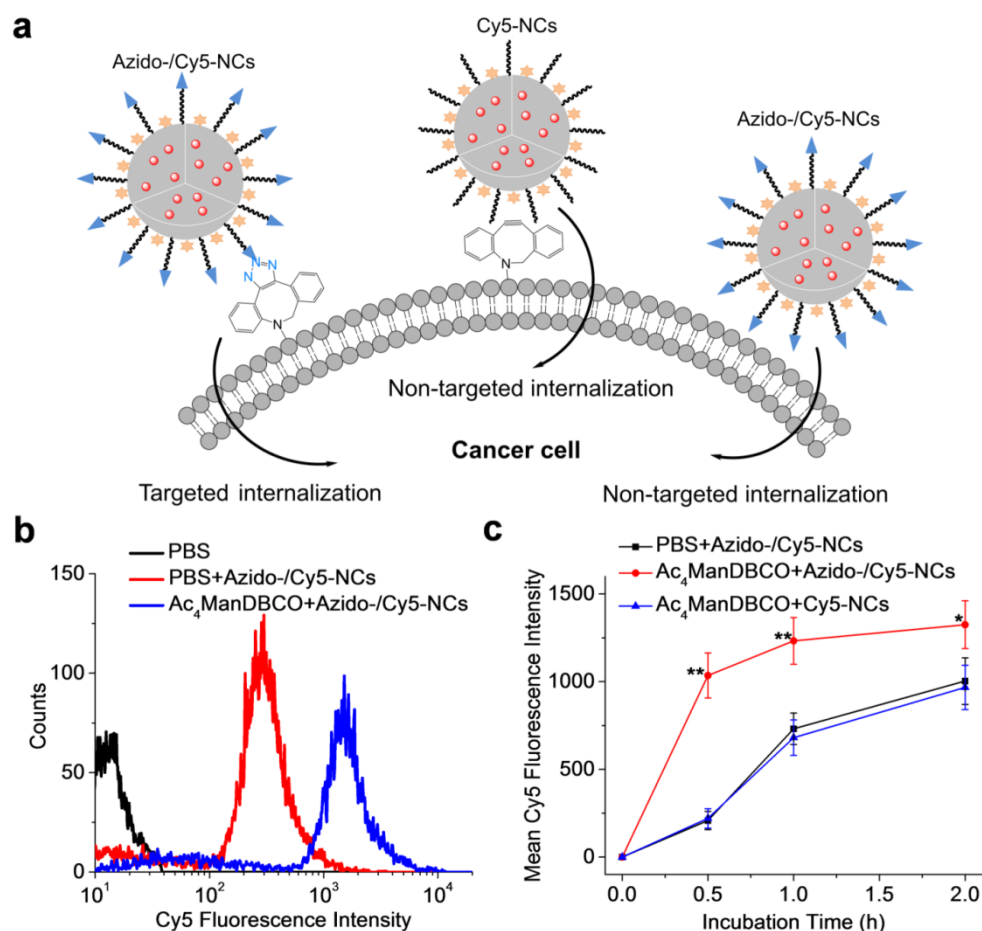
Figure 3. (a) Schematic illustration of the targeted and non-targeted internalization of azido-/Cy5-NCs by cancer cells. (b) Flow cytometry profiles of LS174T cells following treatment with either Ac4ManDBCO (blue curve) or PBS (red curve) for 72 h and further incubation with azido-/Cy5-NCs for 30 min. Cells without azido-/Cy5-NCs treatment served as negative controls (black curve). (c) Mean fluorescence intensity of LS174T cells after incubation with azido-/Cy5-NCs or Cy5-NCs for 0.5, 1, and 2 h, respectively following pre-treatment with Ac4ManDBCO for 72 h. Cells treated with azido-/Cy5-NCs following pretreatment with PBS served as controls (n=6). Statistically significantly lower Cy5 fluorescence intensity than Ac4ManDBCO+azido-/Cy5-NCs group was observed in both PBS+azido-/Cy5-NCs and Ac4ManDBCO+Cy5-NCs groups ($0.01 < *P \le 0.05$, and $0.001 < **P \le 0.01$).

1474

^{64}Cu-/azido-/Cy5-NCs or ^{64}Cu-/Cy5-NCs were i.v. injected and their biodistribution were monitored via PET/CT imaging (Fig. 4a). As shown in Fig. 4b, at 24 h post injection (p.i.) of ^{64}Cu-/azido-/Cy5-NCs, a clear radioactivity contrast was observed between the left tumors pretreated with Ac$_4$ManDBCO and the right tumors pretreated with PBS (Fig. 4b), presumably due to the successful expression of DBCO groups in the left tumors and the resulting improved tumor accumulation of ^{64}Cu-/azido-/Cy5-NCs via *in vivo* Click chemistry. Radioactivity measurement of tissues harvested at 24 h p.i. showed a 1.7-fold accumulation of ^{64}Cu-/azido-/Cy5-NCs in the left tumors pretreated with Ac$_4$ManDBCO compared to the right tumors pretreated with PBS (Fig. 4c). In comparison, accumulation of ^{64}Cu-/Cy5-NCs without azido modification showed negligible difference between the left and right tumors (Fig. 4c), further substantiating the important role of Click chemistry in the observed tumor-targeting effect of ^{64}Cu-/azido-/Cy5-NCs. These findings demonstrated that Ac$_4$ManDBCO could metabolically label LS174T cancer cells with DBCO groups *in vivo* and subsequently mediate cancer-targeted delivery of ^{64}Cu-/azido-/Cy5-NCs via efficient Click chemistry.

Multifunctional silica NCs provide a good platform for multi-modal imaging, such as fluorescence imaging that enables in-depth tracking of NCs within tissues, in addition to PET/CT imaging. We next evaluated the cancer targeting effect of azido-/Cy5-NCs in tumor-bearing athymic nude mice via *in vivo* fluorescence imaging. As shown in Fig. 5a, a noticeable amount of azido-/Cy5-NCs were accumulated in tumors at 6 h p.i., and a clear Cy5 fluorescence contrast was observed between the left tumors pretreated with Ac$_4$ManDBCO and the right tumors pretreated with PBS. The tumor accumulation of azido-/Cy5-NCs drastically increased during 6-24 h, moderately amplified during 24-48 h, and then slightly decreased during 48-72 h, while the significant fluorescence contrast between the left and right tumors remained almost unchanged. It can thus be assumed that, in DBCO-modified tumors, azido-/Cy5-NCs from the bloodstream were attached at a faster rate than in unmodified tumors. That is, a greater amount of NCs were trapped in DBCO-modified tumors than in unmodified tumors within a short time. Active targeting of azido-/Cy5-NCs via Click chemistry was largely completed within 24 h (Fig. 5a), and the passive
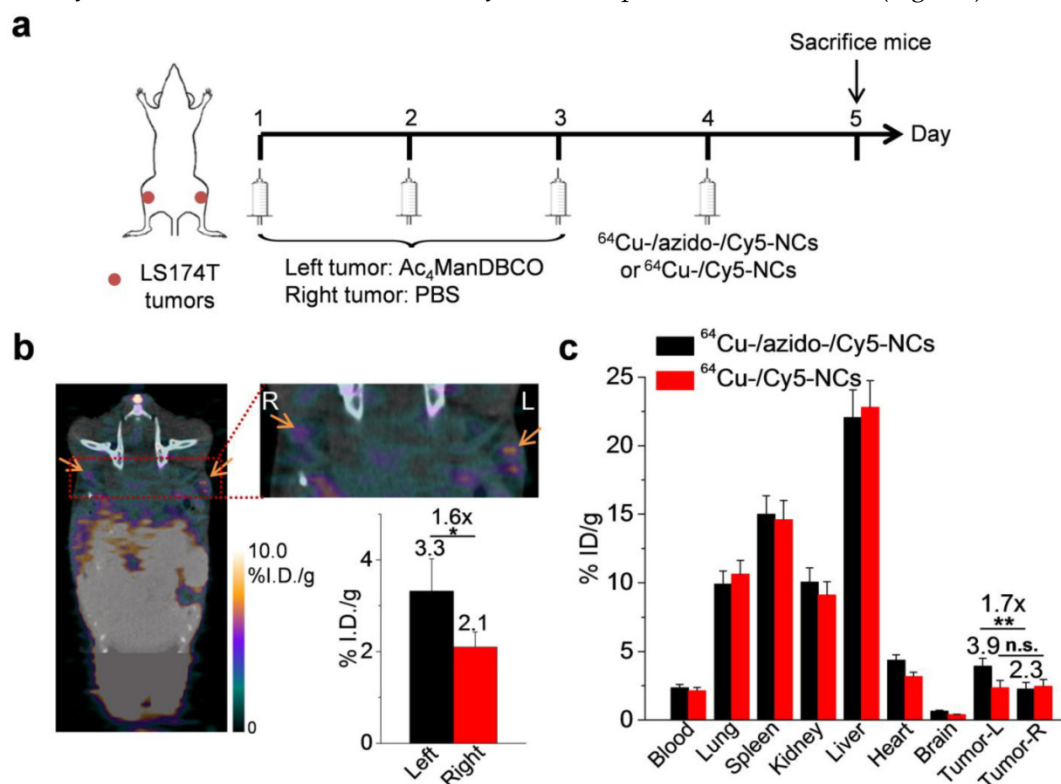
Figure 4. (a) Time frame of *in vivo* imaging study. LS174T tumors were implanted in both flanks of athymic nude mice. When the tumors reached ~50 mm³, Ac$_4$ManDBCO (5 mg/kg) was intratumorally injected into the left tumors once daily for three days (Day 1-3), while the right tumors were injected with PBS as controls. On Day 4, ^{64}Cu-/azido-/Cy5-NCs or ^{64}Cu-/Cy5-NCs (~100 μCi) were i.v. injected and their biodistribution were monitored via PET/CT imaging. (b) PET/CT imaging of athymic nude mouse at 24 h post injection of ^{64}Cu-/azido-/Cy5-NCs. The tumor area was zoomed in to clearly show the retention of ^{64}Cu-/azido-/Cy5-NCs in the left and right tumors. Tumors were shown by the arrows. Inset: calculated radioactivity of the left and right tumors using the imaging software. (c) Biodistribution of ^{64}Cu-/azido-/Cy5-NCs and ^{64}Cu-/Cy5-NCs at 24 h post injection, as determined by *ex vivo* radioactivity measurement on a λ-counter. Data were presented as mean ± SEM (n=3) and analyzed by Student's t-test (two-tailed) (0.001 < **P ≤ 0.01).

penetration and efflux of azido-/Cy5-NCs then reached an equilibrium. *Ex vivo* imaging of tissues harvested at 72 h p.i. of azido-/Cy5-NCs showed a 1.6-fold Cy5 fluorescence intensity in the left tumors compared to the right tumors (Fig. 5b-c). In comparison, Cy5-NCs without azido modification showed minimal fluorescence difference between the left and right tumors (Fig. 5c), which substantiated the essential role of Click chemistry to mediate tumor targeting. In consistence with these quantitative analyses, confocal images of tumor sections also showed much stronger Cy5 fluorescence intensity in the left tumors (Fig. 5e). These results again verified that DBCO-modified tumor cells could significantly improve the tumor accumulation of azido-/Cy5-NCs via *in vivo* Click chemistry.

Conclusion

In conclusion, we demonstrated that Ac$_4$ManDBCO could metabolically label LS174T colon cancer cells with DBCO groups and subsequently mediate the targeted internalization of azido-/Cy5-NCs via Click chemistry *in vitro*. *In vivo* PET/CT and fluorescence dual-modal imaging studies further verified that labeling of LS174T tumors with Ac$_4$ManDBCO could significantly enhance the tumor accumulation of azido-modified silica NCs.

This study, for the first time, demonstrated the feasibility of introducing large-sized DBCO groups onto the surface of cancer cells, which thus enabled the use of small-sized azido groups as the targeting ligand. With this strategy, azido groups can be incorporated into therapeutic agents or nanomedicines at high densities without compromising their physiochemical properties. In principle, the current strategy can also be extended to cancer cell labeling with other large-sized chemical functional groups for subsequent targeted delivery of extracellular materials. With future advances in the development of cancer-selective sugar labeling, the azido-modified silica NCs developed in this study will provide a promising platform for cancer-targeted diagnosis and therapy.
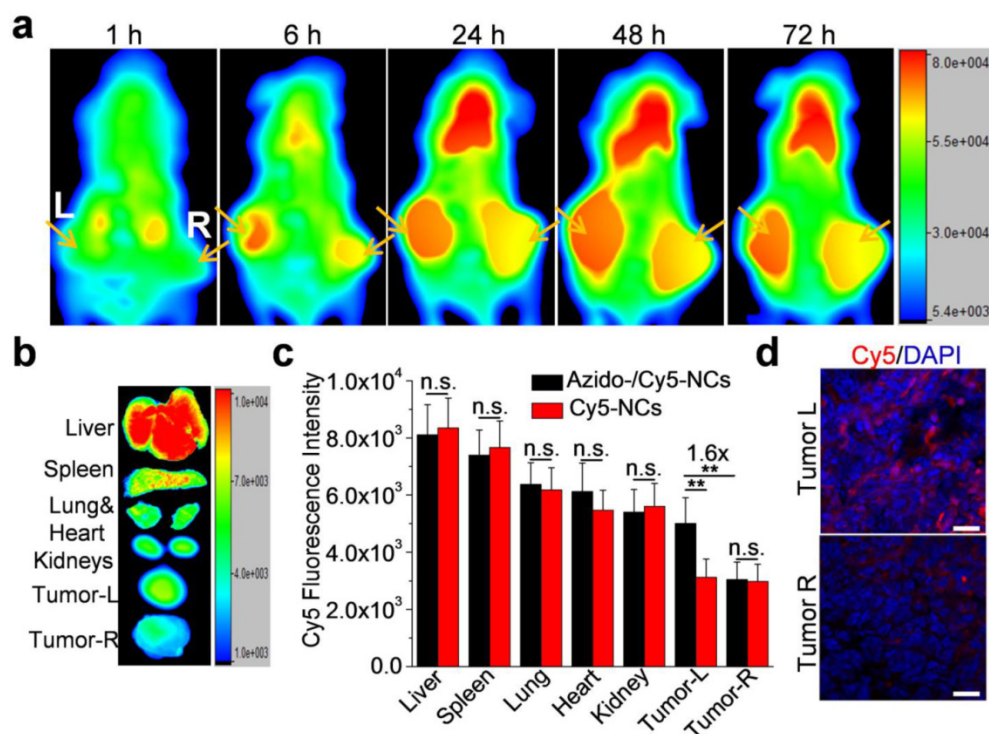
Supplementary Material

Supplementary figures.
http://www.thno.org/v06p1467s1.pdf

Acknowledgements

Figure 5. (a) Whole-body fluorescence imaging of athymic nude mice bearing LS174T tumors at 1, 6, 24, 48, and 72 h post injection of azido-/Cy5-NCs. Tumors were shown by the arrows. The left tumors were injected with Ac$_4$ManDBCO (5 mg/kg) once daily for three days (Day 1-3), while the right tumors were injected with PBS as controls. Azido-/Cy5-NCs or Cy5-NCs were i.v. injected on Day 4. (b) *Ex vivo* imaging of tissues harvested at 72 h post injection of azido-/Cy5-NCs. (c) Mean Cy5 fluorescence intensity of tissues extracted from *ex vivo* images (n=3). (d) Representative CLSM images of tissue sections of the left and right tumors from mice treated with azido-/Cy5-NCs. Cell nuclei were stained with DAPI (blue).

Competing Interests

The authors declare no competing financial interest.

References

1. Alonso MJ. Nanomedicines for overcoming biological barriers. Biomed Pharmacother. 2004;58:168-72.
2. Sumer B, Gao J. Theranostic nanomedicine for cancer. Nanomedicine. 2008; 3: 137-40.
3. Wagner V, Dullaart A, Bock AK, Zweck A. The emerging nanomedicine landscape. Nat Biotechnol. 2006;24:1211-7.
4. Duncan R. Polymer conjugates as anticancer nanomedicines. Nat Rev Cancer. 2006;6:688-701.
5. Wang H, Tang L, Tu C, Song Z, Yin Q, Yin L, Zhang Z, Cheng J. Redox-Responsive, Core-Cross-Linked Micelles Capable of On-Demand, Concurrent Drug Release and Structure Disassembly. Biomacromolecules. 2013;14:3706-12.
6. Tang L, Yang X, Yin Q, Cai K, Wang H, Chaudhury I, Yao C, Zhou Q, Kwon M, Hartman JA, Dobrucki IT, Dobrucki LW, Borst LB, Lezmi S, Helferich WG, Ferguson AL, Fan TM, Cheng J. Investigating the optimal size of anticancer nanomedicine. Proc Natl Acad Sci USA. 2014;111:15344-9.
7. Huang X, Zhang F, Lee S, Swierczewska M, Kiesewetter DO, Lang L, Zhang G, Zhu L, Gao H, Choi HS, Niu G, Chen X. Long-term multimodal imaging of tumor draining sentinel lymph nodes using mesoporous silica-based nanoprobes. Biomaterials. 2012;33:4370-8.
8. Kumar R, Roy I, Ohulchanskky TY, Vathy LA, Bergey EJ, Sajjad M, Prasad PN. In Vivo Biodistribution and Clearance Studies Using Multimodal Organically Modified Silica Nanoparticles. ACS Nano. 2010;4:699-708.
9. Wang L, Wang K, Santra S, Zhao X, Hilliard LR, Smith JE, Wu Y, Tan W. Watching silica nanoparticles glow in the biological world. Anal Chem. 2006;78:646-54.
10. Rieter WJ, Kim JS, Taylor KML, An H, Lin W, Tarrant T, Lin W. Hybrid Silica Nanoparticles for Multimodal Imaging. Angew Chem Int Ed. 2007;46:3680-2.
11. Tang F, Li L, Chen D. Mesoporous silica nanoparticles: synthesis, biocompatibility and drug delivery. Adv Mater. 2012;24:1504-34.
12. Tang L, Fan TM, Borst LB, Cheng J. Synthesis and Biological Response of Size-Specific, Monodisperse Drug–Silica Nanoconjugates. ACS Nano. 2012;6:3954-66.
13. Tang L, Gabrielson NP, Uckun FM, Fan TM, Cheng J. Size-Dependent Tumor Penetration and in Vivo Efficacy of Monodisperse Drug–Silica Nanoconjugates. Mol Pharm. 2013;10:883-92.
14. Tang L, Yang X, Dobrucki LW, Chaudhury I, Yin Q, Yao C, Lezmi S, Helferich WG, Fan TM, Cheng J. Aptamer-Functionalized, Ultra-Small, Monodisperse Silica Nanoconjugates for Targeted Dual-Modal Imaging of Lymph Nodes with Metastatic Tumors. Angew Chem Int Ed. 2012;51:12721-6.
15. Tang L, Cheng J. Nonporous silica nanoparticles for nanomedicine application. Nano Today. 2013;8:290-312.
16. Prescher JA, Dube DH, Bertozzi CR. Chemical remodelling of cell surfaces in living animals. Nature. 2004;430:873-7.
17. Saxon E, Luchansky SJ, Hang HC, Yu C, Lee SC, Bertozzi CR. Investigating cellular metabolism of synthetic azidosugars with the Staudinger ligation. J Am Chem Soc. 2002;124:14893-902.
18. Dube DH, Bertozzi CR. Metabolic oligosaccharide engineering as a tool for glycobiology. Curr Opin Chem Biol. 2003;7:616-25.
19. Saxon E, Bertozzi CR. Chemical and biological strategies for engineering cell surface glycosylation. Annu. Rev. Cell Dev Biol. 2001;17:1-23.
20. Baskin JM, Prescher JA, Laughlin ST, Agard NJ, Chang PV, Miller IA, Lo A, Codelli JA, Bertozzi CR. Copper-free click chemistry for dynamic in vivo imaging. Proc Natl Acad Sci USA. 2007;104:16793-7.
21. Prescher JA, Bertozzi CR. Chemistry in living systems. Nat Chem Biol. 2005;1:13-21.
22. Baskin JM, Bertozzi CR. Bioorthogonal click chemistry: covalent labeling in living systems. Mol Inform. 2007;26:1211-9.
23. Chang PV, Prescher JA, Sletten EM, Baskin JM, Miller IA, Agard NJ, Lo A, Bertozzi CR. Copper-free click chemistry in living animals. Proc Natl Acad Sci USA 2010;107:1821-6.
24. Codelli JA, Baskin JM, Agard NJ, Bertozzi CR. Second-generation difluorinated cyclooctynes for copper-free click chemistry. J Am Chem Soc. 2008;130:11486-93.
25. Laughlin ST, Baskin JM, Amacher SL, Bertozzi CR. In vivo imaging of membrane-associated glycans in developing zebrafish. Science. 2008;320:664-7.
26. Wang H, Gauthier M, Kelly JR, Miller RJ, Xu M, O'Brien WD, Cheng J. Targeted Ultrasound-Assisted Cancer-Selective Chemical Labeling and Subsequent Cancer Imaging using Click Chemistry. Angew Chem Int Ed. 2016;55:1-6.
27. Koo H, Lee S, Na JH, Kim SH, Hahn SK, Choi K, Kwon IC, Jeong SY, Kim K. Bioorthogonal Copper-Free Click Chemistry In Vivo for Tumor-Targeted Delivery of Nanoparticles. Angew Chem Int Ed. 2012;51:11836-40.
28. Campbell-Verduyn LS, Mirfeizi L, Schoonen AK, Dierckx RA, Elsinga PH, Feringa BL. Strain-Promoted Copper-Free "Click" Chemistry for 18F Radiolabeling of Bombesin. Angew Chem Int Ed. 2011;50:11117-20.
29. Xie R, Hong S, Feng L, Rong J, Chen X. Cell-Selective Metabolic Glycan Labeling Based on Ligand-Targeted Liposomes. J Am Chem Soc. 2012;134:9914-7.
30. Bernardin A, Cazet A, Guyon L, Delannoy P, Vinet F, Bonnaffé D, Texier I. Copper-free click chemistry for highly luminescent quantum dot conjugates: application to in vivo metabolic imaging. Bioconjugate Chem. 2010;21:583-8.
31. von Maltzahn G, Ren Y, Park JH, Min DH, Kotamraju VR, Jayakumar J, Fogal V, Sailor MJ, Ruoslahti E, Bhatia SN. In vivo tumor cell targeting with "click" nanoparticles. Bioconjugate Chem. 2008;19:1570-8.
32. Lee S, Koo H, Na JH, Han SJ, Min HS, Lee SJ, Kim SH, Yun SH, Jeong SY, Kwon IC. Chemical tumor-targeting of nanoparticles based on metabolic glycoengineering and click chemistry. ACS Nano. 2014;8:2048-63.
33. Xie R, Dong L, Huang R, Hong S, Lei R, Chen X. Targeted Imaging and Proteomic Analysis of Tumor-Associated Glycans in Living Animals. Angew Chem Int Ed. 2014;53:14082-6.